Subwavelength Grating Metamaterial Racetrack Resonator for Sensing and Modulation

Xiaochuan Xu, *Senior Member, IEEE*, Zeyu Pan, *Student Member, IEEE*, Chi-Jui Chung, Ching-Wen Chang, Hai Yan, and Ray T. Chen, *Fellow, IEEE*

(Invited Paper)

***Abstract*—Subwavelength grating metamaterial racetrack ring resonator (SGMRTR) increases the coupling strength between the bus waveguide and the ring resonator and thus better extinction ratio can be achieved. In this paper, we summarized our recent work on SGMRTRs. We show that with the improved extinction ratio, the intrinsic detection limit of refractive index sensors can be pushed closer to the theoretical limit. We have also demonstrated the first high-speed optical modulator based on electro-optic polymer infiltrated subwavelength grating metamaterial waveguide ring resonator with measured 3-dB bandwidth of 41.4 GHz. The power consumption for digital communication is estimated to be 2.55 *f*J/bit.**

***Index Terms*—Silicon photonics, modulator, silicon-organic hybrid integration, metamaterial, subwavelength grating, sensor.**

I. Introduction

THE advance of modern technologies relies heavily on the discovery and in-depth understanding of materials. While the desire for materials with special properties and quality never fades, "perfect" natural materials for specific applications, unfortunately, do not always exist. Thus, there is substantial interest in tailoring naturally existing materials. The rapid development of nanotechnology provides the ability and the opportunity to engineer materials in nanoscale or even atomic scale and potentially break the limitation of materials on the device performance.

Integrated photonics is one of the areas that artificial materials can significantly improve the performance of devices. Essentially, a typical on-chip circuit is a combination of two or more basic functions, such as photon generation, manipulation (modulation, attenuation, etc.), delivery (waveguiding), and detection. Currently, none of the available material platforms can satisfactorily accomplish all these functions. For instance, silicon photonics enables the high density and low-cost integration of optical components, but it is also well-known that silicon does not favor the generation and manipulation of photons due to its indirect bandgap and absence of second-order nonlinearity. Besides, the high index contrast not only leads to small footprints but also limits the interaction between photons and ambient environment, including electro-optic (EO) polymers and biomolecules.

Subwavelength grating metamaterial (SGM) waveguide, formed by a periodic arrangement of material segments with a pitch less than the wavelength inside the waveguide, provides a method to manipulate many important optical properties such as dispersion and refractive index [1]–[7], and a platform for hybrid integration [8] and sensing [9]–[11]. Recently, it is also used as mechanic suspension structures to break the limitation of material platforms in aspects such as sensitivity and operation wavelength [12]–[14]. SGM was first proposed in 2006 by Cheben, *et al.* as a promising approach to address the light coupling issue of silicon photonics [15]. Despite a large number of reflection interfaces, a propagation loss as low as 2.1 dB/cm was reported, which is comparable with widely used strip waveguides [1]. Innovative components based on the SGM have been showing impressive performance compared to conventional devices [16]–[18]. These demonstrations prove that SGM could potentially address the disadvantages of conventional devices made of naturally existing materials. Motivated by this vision, recent research has been focusing on replicating the success of conventional components with SGM waveguide [8], [11], [16]–[25], such as silicon photonics micro-ring resonators [8], [11], [24], [25]. Compared to conventional strip waveguide, the optical field in SGM waveguides not only exists in the peripheral regions but also between silicon pillars. Thus, higher sensitivity can be expected or enhanced performance in hybrid integration

Manuscript received August 22, 2018; revised September 9, 2018 and April 17, 2019; accepted April 18, 2019. Date of publication May 10, 2019; date of current version May 30, 2019. This work was supported in part by the U.S. Department of Energy (DoE) small business innovative research (SBIR) program under Grant DE SC-0013178, in part by the Air Force Office of Scientific Research (AFOSR) SBIR Program under Grant FA9550-16-C-0033, in part by the Air Force Research Laboratory (AFRL) Small Business Technology Transfer Research (STTR) Program under Grant FA8650-14-C-5006, and in part by the AFOSR Multidisciplinary University Research Initiative (MURI) Program under Grant FA9550-08-1-0394. *(Corresponding author: Xiaochuan Xu.)*

X. Xu is with the Microelectronic Research Center, Department of Electrical and Computer Engineering, University of Texas Austin, Austin, TX 78758 USA, and also with the Omega Optics, Inc., Austin, TX 78757 USA (e-mail: xiaochuan.xu@utexas.edu).

Z. Pan, C.-J. Chung, H. Yan, and R. T. Chen are with the Microelectronic Research Center, Department of Electrical and Computer Engineering, University of Texas Austin, TX 78758 USA (e-mail: panzeyu@utexas.edu; cjchung@utexas.edu; hai.yan@utexas.ed; chen@ece.utexas.edu).

C.-W. Chang is with the Microelectronic Research Center, Department of Electrical and Computer Engineering, University of Texas Austin, Austin, TX 78758 USA, and also with the Department of Physics and Center for Nanoscience and Nanotechnology, National Sun Yat-Sen University, Kaohsiung 80424, Taiwan (e-mail: cwchang@utexas.edu).

Color versions of one or more of the figures in this paper are available online at http://ieeexplore.ieee.org.

Digital Object Identifier 10.1109/JSTQE.2019.2915980

can be achieved. However, the increased interaction inevitably induces additional loss from increased surface roughness and absorption. In addition, the reduced index of SGM does not favor sharp bends and introduces additional radiation loss into the ring due to the wavefront distortion. Although fine tuning the shape of elements of SGM could alleviate the issue, the coupling strength between bus waveguide and resonator must be strengthened to meet critical coupling condition, especially when the cladding of the resonator is absorptive. Junjia Wang *et al.* presented optical filters based on SGM [26], in particular, implementation of Bragg SGMs in silicon-on-insulator (SOI). Micro-ring resonators with extinction ratio (ER) of 23 dB and a quality factor as high as ~20,000 is demonstrated. The ER is further improved to 30 dB using race-track configuration.

In this paper, we summarize our recent progress on SGM racetrack resonators (SGMRTRs) based sensors and modulators. Fundamentally, sensors and modulators can be considered as a transducer which converts index perturbations into detectable optical signals, such as phase and intensity variations, and thus share plenty of similarities. To improve the performance of both types of devices, essentially the interaction between photons and cladding materials needs to be maximized, and at the same time, the quality factor and the ER of the resonator must be maintained at the desired level. Trade-offs are frequently made to balance these design considerations to meet the requirements of various applications.

II. Subwavelength Grating Metamaterial Racetrack Resonator for Sensing Applications

Since the birth of SGM, sensing has been considered as one of its most promising applications [9], [27]–[29]. A comprehensive analysis is provided in [18] which unveils that better sensitivities can be achieved with SGM based sensors compared to conventional strip waveguide based sensors. As mentioned in the previous section, SGMRTRs provide adequate coupling strength to compensate the intrinsic loss of SGM resonators and assure the critical coupling condition can be satisfied. Especially for sensors in absorptive environment, such as aqueous solutions, an ultra-large coupling coefficient is necessary to obtain satisfying ER. In addition, SGMRTRs increase the roundtrip length which subsequently increases the probability for one single molecule to be captured and detected. In this paper, the discussion focuses on the bulk sensitivity but the conclusion can also be applied to surface sensing. To maximize the sensitivity, the SGMRTRs discussed in this section operate with transverse-magnetic (TM) modes instead of the most frequently used transverse-electric (TE) modes. TM modes typically suffer a higher loss in bends, resulting in the increased intrinsic loss within the racetrack resonators.

Fig. 1(a) is the optical microscope image of an SGMRTR in a U-shape configuration, in which a pair of SGM grating couplers were put 250 μm apart to match the pitch of the fiber array. Fig. 1(b) is the scanning electron microscopy (SEM) image of the SGMRTR with the details of SGM grating couplers, strip-to-SGM waveguide converters, and the coupling region shown in Fig. 1(b), (c), and (d), respectively. The strip-to-SGM mode converters were formed by narrowing the waveguide core gradually to 60 nm wide. The length of the converters is 40 μm to reduce the conversion loss [31]. The device was fabricated on SOI with a 220 nm thick silicon device layer and a 3 μm thick buried oxide (BOX) layer. The SGMRTR structures are firstly patterned through electron beam lithography (EBL), followed by the reactive ion etching (RIE). The proximity effect is precompensated to minimize the discrepancy between the design and fabrication.

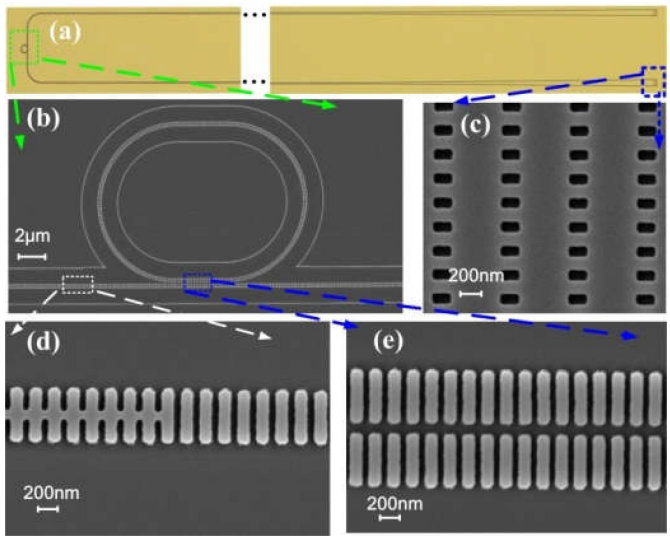

Fig. 1. (a) Optical microscope image of the fabricated SGMRTR with a coupling length of 6.5 μm. (b) SEM image of the SGMRTR (green region in (a)). (c) The TM SGM grating coupler. The magnified SEM images of (d) the left taper between strip waveguide and SGM waveguide in white dashed rectangular region, and (e) the coupling region between the SGM bus waveguide and racetrack resonator in blue dashed rectangular region [30].

To determine the optimum length L_c of the coupling region, a set of SGMRTRs with L_c from 5.5 μm to 7.5 μm with a step of 0.5 μm were fabricated. The SGMRTRs were tested with a broadband source and an optical spectrum analyzer (OSA). The light was guided through one channel of the fiber array to the TM SGM grating coupler and excites the TM mode in the strip waveguide. Output light was collected by another channel in the fiber array. Fig. 2(a) summarizes the collected transmission spectra of SGMRTRs. Fig. 2(b) shows a magnified view of the resonances in the blue box. The resonances were shifted so that each resonance can be distinguished clearly. As seen in Fig. 2(b), the quality factor and the ER of the fabricated SGMRTRs reached their maximum when the coupling length equals 6.5 μm. The full-width at half-maximum (FWHM) of the resonance at 1555.9 nm in DI water is about 0.16 nm, corresponding to a quality factor of ~9800, and the ER is about 24.6 dB.

The bulk sensitivity of the fabricated SGMRTRs with different L_C was characterized by flowing glycerol solution with different concentrations onto the SGMRTRs through microfluidic channels. The chip was kept at 25°C by a temperature controller. The resonance was tracked and plotted in Fig. 3(a). The vertical green dashed line represents the time duration when glycerol solutions with different concentrations were injected.

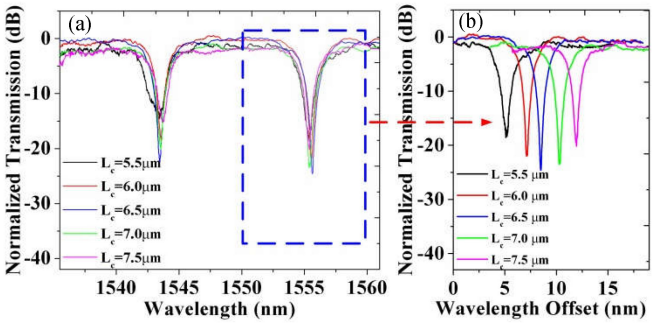

Fig. 2. (a) The transmission spectra of the fabricated five SGMRTRs with $L_c = 5.5\ \mu$m, 6 μm, 6.5 μm, 7 μm, and 7.5 μm, respectively, and DI water cladding. (b) Magnified resonance dips in blue dashed rectangular region in (a). Offsets were added so that each resonance can be seen clearly [30].

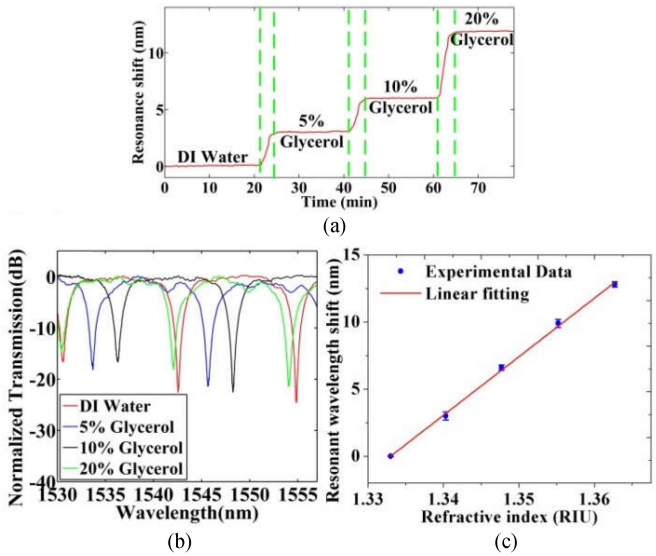

Fig. 3. (a) The time-domain resonance shift of the SGMRTR with $L_c = 6.5\ \mu$m when different concentrations of glycerol solutions (0%, 5%, 10% and 20%) were flowed through the device. (b)The corresponding redshift of the transmission spectra for different concentration glycerol solutions. (c) The linear fitting plot of the resonance shifts [30].

Fig. 3(b) shows the stabilized transmission spectra after the new concentration solutions were applied. The refractive indices for 0%, 5%, 10%, and 20% concentration solutions of glycerol are 1.333, 1.340, 1.347, and 1.362, respectively. Fig. 3(c) is a linear fitting of the resonance shift in relation to the change of the refractive index of the solution. The bulk sensitivity of the SGMRTR is about 429.7 nm/RIU.

The intrinsic detection limitation(*iDL*) of a refractive index sensor is defined as $iDL = \lambda/(S \dot{c} Q)$, which can be considered as the minimum index change required to shift the resonance wavelength by one linewidth ($\Delta\lambda_{3\ \mathrm{dB}}$). S is the sensitivity of the sensor in nm/RIU. Q represents the quality factor. It is obvious that *iDL* is not only determined by the sensitivity but also by the quality factor of the resonator. However, for the racetrack resonators with coupling length between 5.5 and 7.5 μm, the bulk sensitivity remains almost the same. The quality factor, which is a measure of the photon lifetime in the racetrack resonator,

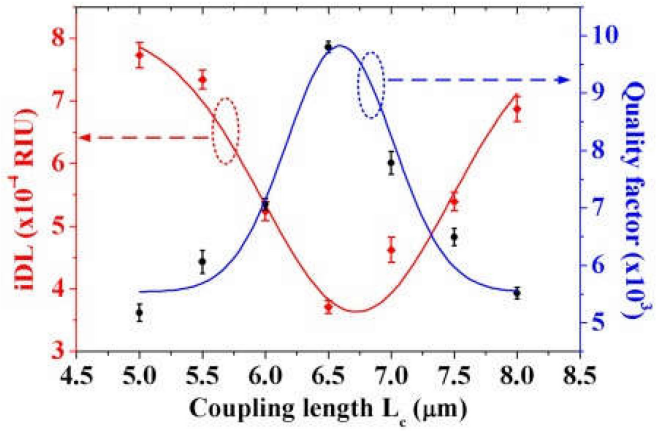

Fig. 4. The *i*DLs and quality factors of the fabricated SGMRTRs with different L_c. The quality factors were measured in DI water [30].

varies significantly as the coupling strength changes. Therefore, we optimized the quality factor of the racetrack resonator to achieve the lowest *i*DL. The *i*DLs and quality factors of the fabricated SGMRTRs with different L_c are shown in Fig. 4. It can be seen from the figure (Gaussian fit of quality factor and *i*DL for different L_c) that the minimum *i*DL can be achieved when the coupling length equals 6.5 μm and the Q is maximized. Through coupling region optimization, a minimum *i*DL of 3.71×10^{-4} was demonstrated. The *i*DL is 32.5% lower than that in the TE circular ring resonator of 5.5×10^{-4} RIU [27], [28]. The sensitivity of the SGMRTR is also better than that of TM mode strip waveguide ring resonators with waveguide thicknesses of 150 nm (247 nm/RIU) and 220 nm (238 nm/RIU) [27]. As indicated in Ref. [10], the sensitivity can be further improved by optimizing the dimensions of the silicon pillars.

III. High Speed Subwavelength Grating Metamaterial Hybrid Modulator

Silicon photonics has been receiving considerable attention due to its potential of leveraging semiconductor manufacture technology to massively produce integrated photonic circuits at a low cost [32]–[34]. However, as aforementioned, silicon is also known for its lack of $\chi^{(2)}$-nonlinearity because of the centrosymmetric lattice structure. The inversion symmetry could possibly be broken by either strain [35], [36] or voltage [37], [38], but the operating voltage is too high for on-chip applications. Thus, efficiently modulating photons on silicon chips with small device footprint is not trivial. Many approaches have been explored to address the challenge [33], [34], such as Pockels effect [39], electro-absorption(known as Franz-Keldysh effect in bulk semiconductor material and the quantum confined stark effect in quantum-well structures) [40], [41], and plasma dispersion effect [42]–[44]. Plasma dispersion effect is one of the most promising candidates [42]–[44], but it not only modulates the phase but also the intensity, leading to a nonlinear response. Although more than 50 Gb/s on-off keying (OOK) has been reported recently [45], further reducing footprint and power consumption while continuously increasing modulation

speed becomes challenging due to the nature of the modulation mechanism [46]. Thus, hybrid integration is a compelling alternative.

Among all hybrid integrable materials [47], EO polymer is particularly attractive because of its ultrahigh EO coefficient ($r_{33} > 500$ pm/V) [48], ultrafast response speed (<1 *f*s) [49], [50], small wavelength dispersion, and spin-casting compatibility. These properties can potentially improve device performance in multiple aspects, including power consumption, modulation speed, and fabrication complexity. Thus, silicon-organic hybrid (SOH) modulator is proposed and studied in the hope of combining the best of the two materials. In SOH platform, one critical issue is that the footprint of SOH modulators is relatively large [51]–[53], which not only significantly reduces integration density but also prevents further improving energy efficiency because of the large capacitance. For example, SOH modulators with bandwidth over 100 GHz have been reported [44], [46], but the millimeter-long phase shifter compromises the integration density. Slow light, such as slot photonic crystals [54], [55], and plasmonic devices [39], [56], is frequently used to effectively shrink the phase shifter length but at the price of significantly increased insertion loss [57]–[61]. In light of silicon microring resonators, there is growing interest in building ring resonance structures on the SOH platform [62]. Many waveguide structures have been studied [63]–[69]. Strip waveguide based microring resonators with EO polymer as top cladding has a radius of 40 μm [63], [70]. The performance of the devices is limited by the small overlap between EO polymer and the guided mode [63], [70]. Slot waveguide based ring resonators can increase the mode volume overlap significantly but suffer from an ultra-high loss of 35 dB/cm [62], [71]. The diameter of the slot waveguide based ring resonator is as large as 60 μm [62]. These results demonstrate that it is challenging to achieve compactness, intense photon-matter interaction(large mode-volume overlap factor), and low insertion loss simultaneously with conventional waveguide structures. In this section, we introduce our recent demonstration of the SGMRTR modulator which achieves >40 GHz bandwidth and a compact footprint [8].

Fig. 5 shows the structure of the SGMRTR [7], which is formed by a rectangular racetrack resonator with four rounded corners side-coupled to an SGM bus waveguide. The shape of the racetrack resonator is defined by the coupling length L_c, phase shifter length L_a, and bending radius *R*, which are 9 μm, 50 μm, and 10 μm, respectively. The four 90° bends at the corners are made of trapezoidal shape pillars to minimize the bending loss [11]. The modulator is fabricated on SOI with 220 nm Silicon and 3 μm BOX. EO polymer SEO125 (Soluxra LLC) is applied as the top cladding. To ensure the SGM structure operates in the subwavelength regime, the period is selected to be 250 nm, and the silicon segment length is 175 nm, corresponding to a duty cycle of 0.7. The width of silicon pillars is 500 nm, which equals the width of the strip waveguide to assure a lossless transition from strip waveguide to SGM mode and vice versa. The mode volume overlap with EO polymer is 36.2%, which is equivalent to $\sim$ nine times of the value of typical strip waveguides($\sim$4.0%). SGM grating couplers were exploited to interface single mode fibers [21], [22]. A rounded rectangular shape is leveraged to enhance the coupling strength between the bus waveguide and the racetrack resonator and thus assure high ER can be achieved. As shown in Fig. 5, due to the compact size, the walk-off between electrical and optical signal is negligible. Thus, high speed modulation can be readily achieved with lumped electrodes. It has been proved that without 50 Ohm termination, lumped electrodes can effectively reduce the power consumption compared to traveling wave electrodes. The central width, gold thickness, and gap of the electrodes are 25 μm, 2.4 μm, and 4 μm, respectively. The SEM pictures of the fabricated SGMRTR are shown as the insets of Fig. 5.

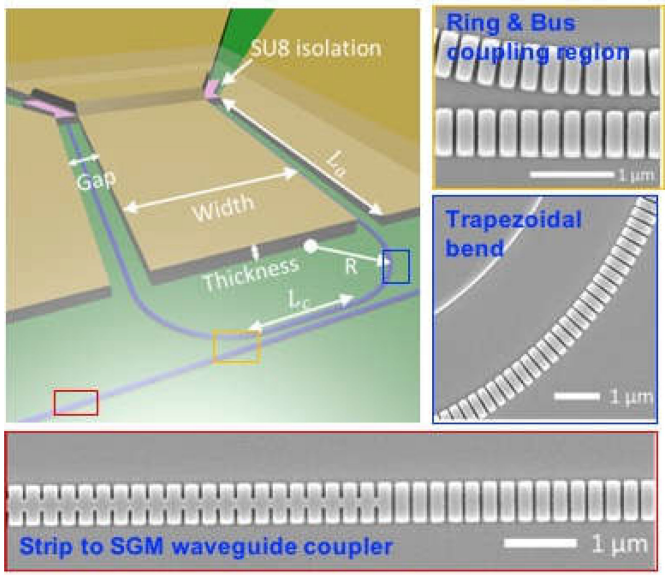

Fig. 5. Schematic of the SOH SGMRTR modulator, which is formed by an SGM racetrack resonator side coupled with SGM bus waveguide. The device is fabricated on SOI platform. Grating couplers are used to couple light into and out of the modulator. Yelow: the coupling region between the racetrack and the bus waveguide. Blue: The trapezoid SGM is used in bends at the four corners to reduce bending loss so that a high quality factor can be achieved. Red: mode converter is employed to convert the mode of conventional strip waveguide into SGM mode and vice versa [8].

The transmission of the fabricated SGMRTR was also characterized by a broadband source and optical spectrum analyzer. To optimize the gap between bus waveguide and the ring, a set of devices with different gaps were fabricated and measured to experimentally optimize the coupling strength. The transmission spectra are summarized in Fig. 6(a). The maximum ER is 27.9 dB, corresponding to an edge-to-edge gap of 500 nm between the bus waveguide and the racetrack resonator. The EO polymer is poled at 150 °C to align chromophore molecules. To characterize the poling efficiency, DC voltage was applied on the electrodes with a configuration shown in the inset of Fig. 6(b). The redshift of the resonance was observed and plotted in Fig. 6(b). The average resonance shift of 41.28 pm/V is observed. Thus, from the EO effect $\Delta n = \frac{1}{2} r_{33} n^3$, the EO coefficient r_{33} is estimated to be 54.7 pm/V, corresponding to a poling efficiency of 43.8% compared to the EO coefficient of the bulk EO polymer.

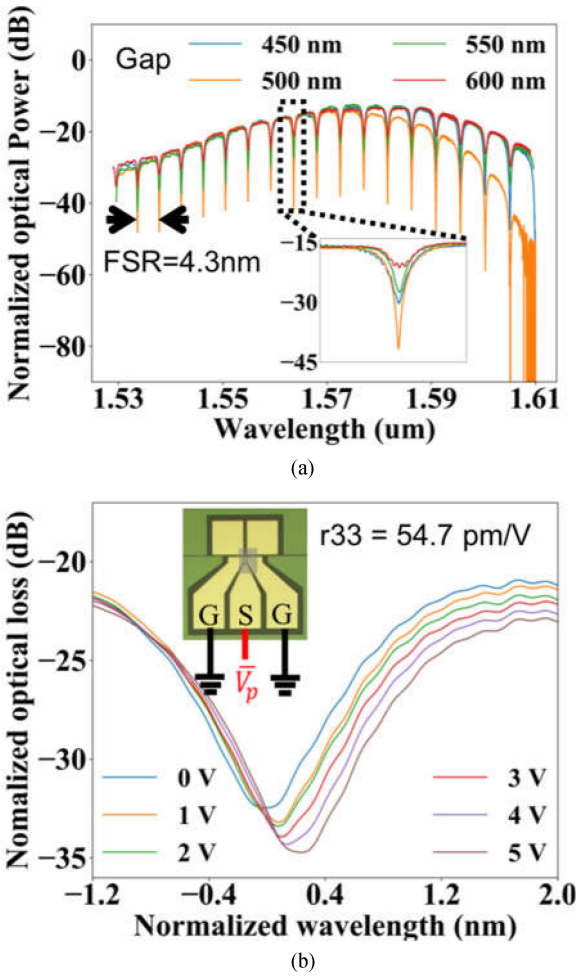

Fig. 6. (a) The normalized optical spectra when the gap between racetrack resonator and bus waveguide equals 450 nm, 500 nm, 550 nm and 600 nm. Inset: the magnified view of resonances between 1.56 and 1.57 μm. (b) The resonance shift when different voltages are applied between the electrodes. Inset: the electrode configuration of static testing [8].

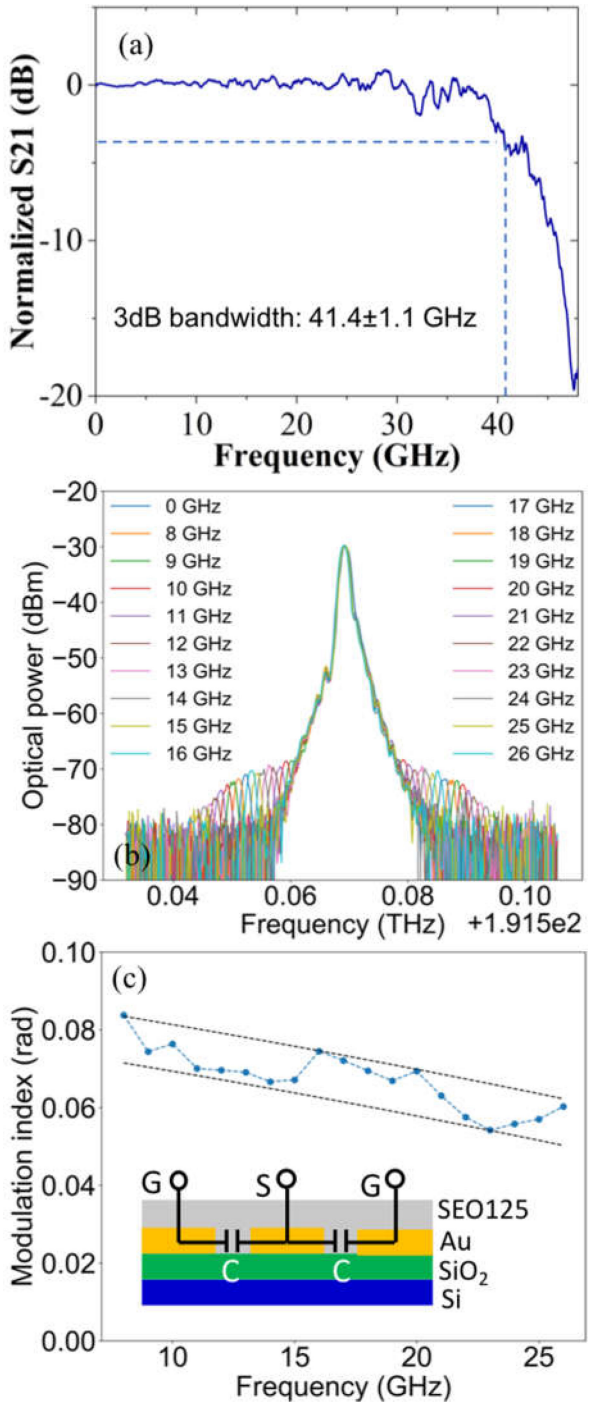

Fig. 7. (a) The measured and normalized optical response versus the frequency. (b) The measured optical transmission spectra of the modulator operating at 8–26 GHz. (c) The modulation index versus frequency. The modulation index results are normalized to a 10 dBm launched power. The equivalent circuit of the modulator is shown in the insert of (c) [8].

The normalized small signal S21 response of the SGM-RTR modulator is shown in Fig. 7(a). The 3-dB bandwidth is 41.4 GHz. The RF bandwidth was further verified by sidelobe detection in the optical domain and the corresponding modulation index. The measured optical transmission spectra of the modulator operating at 8–26 GHz are shown in Fig. 7(b). The modulation index versus frequency is shown in Fig. 7(c). The modulation index is normalized to a 10 dBm launch power. The equivalent circuit of the modulator is shown in the inset of Fig. 7(c). Since lumped electrodes are exploited, the power consumption is equivalent to charging and discharging two capacitors. The total capacitance is estimated to be 0.40 fF. According to Fig. 7(c), assuming $V_{pp} = 5$ V is selected, which corresponds to a 6 dB on-off ratio, the power consumption of non-return-to-zero (NRZ) modulation scheme can be estimated as $CV^2/4 = 2.55$ fJ/bit. The performance of the modulator can be further improved by increasing the poling efficiency and shrinking the size of the resonator. The poling efficiency is limited by the electrical field intensity. Due to the rough sidewalls of the electrodes, the electrical field intensity must be kept low to avoid breakdown, which leads to relatively small poling efficiency. Besides, the EO polymer in the gap between silicon pillars may not be poled effectively because the electric field intensity decreases in this region as silicon is typically doped. The device footprint can be reduced further by using shorter phase shifters.

IV. Conclusion

In this paper, we summarize the recent progress of SGMRTR based devices. The extended coupling region in SGMRTRs can increase the ER and thus improve the iDL of SGMRTR based sensors. SOH modulator with 41.4 GHz bandwidth and 2.55 *f*J/bit power consumption has also been demonstrated. These results prove that SGMRTR is a promising vessel for hybrid integration and sensing. The sensitivity of SGM based devices including SGMRTR can be further improved by optimizing the dimensions of SGM [9], yet the maximum overlap factor is ultimately limited by the asymmetricity of the material platform. This limitation can possibly be solved by increasing the symmetricity such as undercut etching and adding an overlay. In addition to sensing, SGM can also be used for applications requiring high optical intensity. For example, infiltrating SGM with third-order nonlinear materials could generate energy effective all-optical components. Another opportunity is to study the possibility of tuning both electrical and optical properties simultaneously with the same SGM structure. For instance, the minority carrier recombination in SOI relies heavily on surface recombination, resulting in slow recombination rate. Therefore, the carrier injection modulator and two-photon-absorption based devices typically have limited speed. With much the significantly larger surface-to-volume ratio, SGM could possibly yield a new category of high speed and energy efficient devices.

References

[1] P. J. Bock *et al.*, "Subwavelength grating periodic structures in silicon-on-insulator: A new type of microphotonic waveguide," *Opt. Express*, vol. 18, no. 19, pp. 20251–20262, Sep. 13, 2010.

[2] P. Cheben, R. Halir, J. H. Schmid, H. A. Atwater, and D. R. Smith, "Subwavelength integrated photonics," *Nature*, vol. 560, no. 7720, pp. 565–572, Aug. 30, 2018.

[3] P. Cheben *et al.*, "Refractive index engineering with subwavelength gratings for efficient microphotonic couplers and planar waveguide multiplexers," *Opt. Lett.*, vol. 35, no. 15, pp. 2526–2528, Aug. 1, 2010.

[4] D. Benedikovic *et al.*, "Dispersion control of silicon nanophotonic waveguides using sub-wavelength grating metamaterials in near- and mid-IR wavelengths," *Opt. Express*, vol. 25, no. 16, pp. 19468–19478, Aug. 7, 2017.

[5] D. Benedikovic *et al.*, "L-shaped fiber-chip grating couplers with high directionality and low reflectivity fabricated with deep-UV lithography," *Opt. Lett.*, vol. 42, no. 17, pp. 3439–3442, Sep. 1, 2017.

[6] X. C. Xu, C. J. Chung, Z. Y. Pan, H. Yan, and R. T. Chen, "Periodic waveguide structures for on-chip modulation and sensing," *Japanese J. Appl. Phys.*, vol. 57, no. 8, Aug. 2018.

[7] D. Oser *et al.*, "Subwavelength engineering and asymmetry: Two efficient tools for sub-nanometer-bandwidth silicon Bragg filters," *Opt. Lett.*, vol. 43, no. 14, pp. 3208–3211, Jul. 15, 2018.

[8] Z. Y. Pan *et al.*, "High-speed modulator based on electro-optic polymer infiltrated subwavelength grating waveguide ring resonator," *Laser Photon. Rev.*, vol. 12, no. 6, Jun. 2018, Art. no. 1700300.

[9] J. G. Wangueemert-Perez *et al.*, "Evanescent field waveguide sensing with subwavelength grating structures in silicon-on-insulator," *Opt. Lett.*, vol. 39, no. 15, pp. 4442–4445, Aug. 1, 2014.

[10] J. G. Wanguemert-Perez *et al.*, "Subwavelength structures for silicon photonics biosensing," *Opt. Laser Technol.*, vol. 109, pp. 437–448, Jan. 2019.

[11] H. Yan *et al.*, "Unique surface sensing property and enhanced sensitivity in microring resonator biosensors based on subwavelength grating waveguides," *Opt. Express*, vol. 24, no. 26, pp. 29725–29734, Dec. 26, 2016.

[12] W. Zhou, Z. Z. Cheng, X. R. Wu, X. K. Sun, and H. K. Tsang, "Fully suspended slot waveguide platform," *J. Appl. Phys.*, vol. 123, no. 6, Feb. 14, 2018, Art. no. 063103.

[13] J. S. Penades *et al.*, "Suspended SOI waveguide with sub-wavelength grating cladding for mid-infrared," *Opt. Lett.*, vol. 39, no. 19, pp. 5661–5664, Oct. 1, 2014.

[14] J. S. Penades *et al.*, "Suspended silicon mid-infrared waveguide devices with subwavelength grating metamaterial cladding," *Opt. Express*, vol. 24, no. 20, pp. 22908–22916, Oct. 3, 2016.

[15] P. Cheben, D. X. Xu, S. Janz, and A. Densmore, "Subwavelength waveguide grating for mode conversion and light coupling in integrated optics," *Opt. Express*, vol. 14, no. 11, pp. 4695–4702, May 29, 2006.

[16] R. Halir *et al.*, "Waveguide sub-wavelength structures: A review of principles and applications," *Laser Photon. Rev.*, vol. 9, no. 1, pp. 25–49, Jan. 2015.

[17] R. Halir *et al.*, "Recent advances in silicon waveguide devices using subwavelength gratings," *IEEE J. Sel. Topics Quantum Electron.*, vol. 20, no. 4, Jul./Aug. 2014, Art. no. 8201313.

[18] L. R. Chen, "Subwavelength grating waveguide devices in silicon-on-insulators for integrated microwave photonics," *Chin. Opt. Lett.*, vol. 15, no. 1, Jan. 10, 2017, Art. no. 010004.

[19] R. Halir *et al.*, "Ultra-broadband nanophotonic beamsplitter using an anisotropic sub-wavelength metamaterial," *Laser Photon. Rev.*, vol. 10, no. 6, pp. 1039–1046, Nov, 2016.

[20] R. Halir *et al.*, "Waveguide grating coupler with subwavelength microstructures," *Opt. Lett.*, vol. 34, no. 9, pp. 1408–1410, May 1, 2009.

[21] X. C. Xu *et al.*, "Colorless grating couplers realized by interleaving dispersion engineered subwavelength structures," *Opt. Lett.*, vol. 38, no. 18, pp. 3588–3591, Sep. 15, 2013.

[22] X. C. Xu *et al.*, "Complementary metal-oxide-semiconductor compatible high efficiency subwavelength grating couplers for silicon integrated photonics," *Appl. Phys. Lett.*, vol. 101, no. 3, Jul. 16, 2012, Art. no. 031109.

[23] J. Ctyroky *et al.*, "Design of narrowband Bragg spectral filters in subwavelength grating metamaterial waveguides," *Opt. Express*, vol. 26, no. 1, pp. 179–194, Jan. 8, 2018.

[24] V. Donzella *et al.*, "Design and fabrication of SOI micro-ring resonators based on sub-wavelength grating waveguides," *Opt. Express*, vol. 23, no. 4, pp. 4791–4803, Feb. 23, 2015.

[25] Z. Wang, X. C. Xu, D. L. Fan, Y. G. Wang, and R. T. Chen, "High quality factor subwavelength grating waveguide micro-ring resonator based on trapezoidal silicon pillars," *Opt. Lett.*, vol. 41, no. 14, pp. 3375–3378, Jul. 15, 2016.

[26] J. J. Wang, I. Glesk, and L. R. Chen, "Subwavelength grating filtering devices," *Opt. Express*, vol. 22, no. 13, pp. 15335–15345, Jun. 30, 2014.

[27] X. Xu, "Silicon nanomembrane for high performance conformal photonic devices," Ph.D. dissertation, Elect. Comput. Eng., The Univ. Texas at Austin Austin, Austin, TX, USA, 2013.

[28] P. Cheben *et al.*, *Composite Subwavelength-Structured Waveguide in Optical Systems*, 2013.

[29] V. Donzella *et al.*, "Sub-wavelength grating components for integrated optics applications on SOI chips," *Opt. Express*, vol. 22, no. 17, pp. 21037–21050, Aug. 25, 2014.

[30] L. J. Huang *et al.*, "Improving the detection limit for on-chip photonic sensors based on subwavelength grating racetrack resonators," *Opt. Express*, vol. 25, no. 9, pp. 10527–10535, May 1, 2017.

[31] P. J. Bock *et al.*, "Subwavelength grating crossings for silicon wire waveguides," *Opt. Express*, vol. 18, no. 15, pp. 16146–16155, Jul. 19, 2010.

[32] R. A. Soref, "Silicon-based optoelectronics," *Proc. IEEE*, vol. 81, no. 12, pp. 1687–1706, Dec. 1993.

[33] R. Soref, "The past, present, and future of silicon photonics," *IEEE J. Sel. Topics Quantum Electron.*, vol. 12, no. 6, pp. 1678–1687, Nov./Dec. 2006.

[34] D. Thomson *et al.*, "Roadmap on silicon photonics," *J. Opt.*, vol. 18, no. 7, Jul. 2016, Art. no. 073003.

[35] M. Borghi *et al.*, "High-frequency electro-optic measurement of strained silicon racetrack resonators," *Opt. Lett.*, vol. 40, no. 22, pp. 5287–5290, Nov. 15, 2015.

[36] C. Schriever *et al.*, "Second-order optical nonlinearity in silicon waveguides: Inhomogeneous stress and interfaces," *Adv. Opt. Mater.*, vol. 3, no. 1, pp. 129–136, 2015.

[37] M. Berciano *et al.*, "Fast linear electro-optic effect in a centrosymmetric semiconductor," *Commun. Phys.*, vol. 1, Oct. 12, 2018, Art. no. 64.

[38] E. Timurdogan, C. V. Poulton, M. J. Byrd, and M. R. Watts, "Electric field-induced second-order nonlinear optical effects in silicon waveguides," *Nature Photon.*, vol. 11, no. 3, pp. 200–206, Mar. 2017.

[39] C. Koos *et al.*, "Silicon-organic hybrid (SOH) and plasmonic-organic hybrid (POH) integration," *J. Lightw. Technol.*, vol. 34, no. 2, pp. 256–268, Jan. 15, 2016.

[40] L. Mastronardi *et al.*, "High-speed Si/GeSi hetero-structure electro absorption modulator," *Opt. Express*, vol. 26, no. 6, pp. 6663–6673, Mar. 19, 2018.
[41] D. Z. Feng *et al.*, "High speed GeSi electro-absorption modulator at 1550 nm wavelength on SOI waveguide," *Opt. Express*, vol. 20, no. 20, pp. 22224–22232, Sep. 24, 2012.
[42] R. Ding *et al.*, "High-speed silicon modulator with slow-wave electrodes and fully independent differential drive," *J. Lightw. Technol.*, vol. 32, no. 12, pp. 2240–2247, Jun. 15, 2014.
[43] R. Ding *et al.*, "Design and characterization of a 30-GHz bandwidth low-power silicon traveling-wave modulator," *Opt. Commun.*, vol. 321, pp. 124–133, Jun. 15, 2014.
[44] H. Xu *et al.*, "Demonstration and characterization of high-speed silicon depletion-mode mach-zehnder modulators," *IEEE J. Sel. Topics Quantum Electron.*, vol. 20, no. 4, Jul./Aug. 2014, Art. no. 3400110.
[45] D. J. Thomson *et al.*, "50-Gb/s silicon optical modulator," *IEEE Photon. Technol. Lett.*, vol. 24, no. 4, pp. 234–236, Feb. 15, 2012.
[46] L. Alloatti *et al.*, "100 GHz silicon-organic hybrid modulator," *Light-Sci. Appl.*, vol. 3, May. 2014, Art. no. e173.
[47] D. Perez-Galacho *et al.*, "Low voltage 25 Gbps silicon Mach-Zehnder modulator in the O-band," *Opt. Express*, vol. 25, no. 10, pp. 11217–11222, May 15, 2017.
[48] W. Heni *et al.*, "Nonlinearities of organic electro-optic materials in nanoscale slots and implications for the optimum modulator design," *Opt. Express*, vol. 25, no. 3, pp. 2627–2653, Feb. 6, 2017.
[49] B. Bortnik *et al.*, "Electrooptic polymer ring resonator modulation up to 165 GHz," *IEEE J. Sel. Topics Quantum Electron.*, vol. 13, no. 1, pp. 104–110, Jan./Feb. 2007.
[50] D. T. Chen *et al.*, "Demonstration of 110 GHz electro-optic polymer modulators," *Appl. Phys. Lett.*, vol. 70, no. 25, pp. 3335–3337, Jun. 23, 1997.
[51] P. Cheben, J. Bock Przemek, Jen H Schmid, Dan-Xia XuAdam Densmore, S. Janz *et al.*, "Silicon-organic hybrid (SOH) modulators for intensity-modulation / direct-detection links with line rates of up to 120 Gbit/s," *Opt. Express*, vol. 25, no. 20, pp. 23784–23800, Oct. 2, 2017.
[52] C. Kieninger *et al.*, "Record-high in-device electro-optic coefficient of 359 pm/V in a silicon-organic hybrid (SOH) modulator," *presented at the OSA Tech. Dig. (online)*, San Jose, CA, USA, 2017, Paper STu3N.2.
[53] H. Zwickel *et al.*, "100 Gbit/s serial transmission using a silicon-organic hybrid (SOH) modulator and a duobinary driver IC," presented at the Optical Fiber Communications Conf. and Exhibition, Los Angeles, CA, USA, 2017, Paper W4I.5.
[54] J. M. Brosi *et al.*, "High-speed low-voltage electro-optic modulator with a polymer-infiltrated silicon photonic crystal waveguide," *Opt. Express*, vol. 16, no. 6, pp. 4177–4191, Mar. 17, 2008.
[55] X. Y. Zhang *et al.*, "High performance optical modulator based on electro-optic polymer filled silicon slot photonic crystal waveguide," *J. Lightw. Technol.*, vol. 34, no. 12, pp. 2941–2951, Jun. 15, 2016.
[56] A. Melikyan *et al.*, "High-speed plasmonic phase modulators," *Nature Photon.*, vol. 8, no. 3, pp. 229–233, Mar. 2014.
[57] H. Yan *et al.*, "One-dimensional photonic crystal slot waveguide for silicon-organic hybrid electro-optic modulators," *Opt. Lett.*, vol. 41, no. 23, pp. 5466–5469, Dec. 1, 2016.
[58] R. Palmer *et al.*, "High-speed, low drive-voltage silicon-organic hybrid modulator based on a binary-chromophore electro-optic material," *J. Lightw. Technol.*, vol. 32, no. 16, pp. 2726–2734, Aug. 15, 2014.
[59] R. Palmer *et al.*, "Silicon-organic hybrid MZI modulator generating OOK, BPSK and 8-ASK signals for Up to 84 Gbit/s," *IEEE Photon. J.*, vol. 5, no. 2, Apr. 2013, Art. no. 6600907.
[60] R. Ding *et al.*, "Demonstration of a low V pi L modulator with GHz bandwidth based on electro-optic polymer-clad silicon slot waveguides," *Opt. Express*, vol. 18, no. 15, pp. 15618–15623, Jul. 19, 2010.
[61] T. Baehr-Jones *et al.*, "Nonlinear polymer-clad silicon slot waveguide modulator with a half wave voltage of 0.25 V," *Appl. Phys. Lett.*, vol. 92, no. 16, Apr. 21, 2008, Art. no. 163303.
[62] M. Gould *et al.*, "Silicon-polymer hybrid slot waveguide ring-resonator modulator," *Opt. Express*, vol. 19, no. 5, pp. 3952–3961, Feb. 28, 2011.
[63] J. Takayesu *et al.*, "A hybrid electrooptic microring resonator-based 1 x 4 x 1 ROADM for wafer scale optical interconnects," *J. Lightw. Technol.*, vol. 27, no. 1–4, pp. 440–448, Jan./Feb. 2009.
[64] X. Sun, D. X. Dai, L. Thylen, and L. Wosinski, "Double-slot hybrid plasmonic ring resonator used for optical sensors and modulators," *Photonics*, vol. 2, no. 4, pp. 1116–1130, Dec. 2015.
[65] P. Steglich *et al.*, "Novel ring resonator combining strong field confinement with high optical quality factor," *IEEE Photon. Technol. Lett.*, vol. 27, no. 20, pp. 2197–2200, Oct. 15, 2015.
[66] P. Rabiei, W. H. Steier, C. Zhang, and L. R. Dalton, "Polymer micro-ring filters and modulators," *J. Lightw. Technol.*, vol. 20, no. 11, pp. 1968–1975, Nov., 2002.
[67] F. Qiu *et al.*, "Ultra-thin silicon/electro-optic polymer hybrid waveguide modulators," *Appl. Phys. Lett.*, vol. 107, no. 12, Sep. 21, 2015, Art. no. 123302.
[68] F. Y. Gardes *et al.*, "High-speed modulation of a compact silicon ring resonator," in *Proc. 6th IEEE Int. Conf. Group IV Photon.*, 2002, pp. 241–243.
[69] T. Baba *et al.*, "50-Gb/s ring-resonator-based silicon modulator," *Opt. Express*, vol. 21, no. 10, pp. 11869–11876, May 20, 2013.
[70] J. M. Lee, D. J. Kim, H. Ahn, S. H. Park, and G. Kim, "Temperature dependence of silicon nanophotonic ring resonator with a polymeric overlayer," *J. Lightw. Technol.*, vol. 25, no. 8, pp. 2236–2243, Aug. 2007.
[71] M. Lauermann *et al.*, "Low-power silicon-organic hybrid (SOH) modulators for advanced modulation formats," *Opt. Express*, vol. 22, no. 24, pp. 29927–29936, Dec. 1, 2014.

Xiaochuan Xu (SM'15) received the B.S. and M.S. degrees in electrical engineering from the Harbin Institute of Technology, Harbin, China, in 2006 and 2009, respectively, and the Ph.D. degree in electrical and computer engineering from the University of Texas, Austin, TX, USA, in 2013. He has authored and coauthored more than 100 peer-reviewed journal and conference papers, and holds three U.S. patents. He also served as principle investigators of multiple small business innovation research (SBIR) and small business technology transfer research (STTR) programs supported by Air Force, NASA, DoE, and NIH. His current research interests include flexible photonics, nonlinear optics, fiber optics, and silicon photonics. He is a senior member of IEEE, and a member of OSA and SPIE.

Zeyu Pan (S'12) received the B.S. degree in optical information science and technology from the Nanjing University of Science and Technology, Nanjing, China, in 2010, and the M.S. degree in electrical and computer engineering from the University of Alabama in Huntsville, Huntsville, AL, USA, in 2013. He is currently working toward the Ph.D. degree with the University of Texas at Austin, Austin, TX, USA. He has authored and coauthored about 38 journal and conference publications. His interests include the polymer waveguide, printed flexible electronics and photonics, patch array antennas, thermo- and electrooptic polymers, phase delay, nanofabrication, RF measurements, inkjet printing, imprinting, and numerical algorithm.

Chi-Jui Chung received the B.S. degree in mechanical engineering from National Chiao Tung University, Hsinchu, Taiwan, in 2009, and the M.S. degree in power mechanical engineering from National Tsing Hua University, Hsinchu, Taiwan, in 2011. He is currently working toward the Ph.D. degree with the University of Texas at Austin, Austin, TX, USA. From 2011 to 2014, he was with the Electronics and Opto-Electronics Research Laboratories, Industrial Technology Research Institute, Hsinchu, Taiwan. His current research interests include subvolt photonic crystal waveguide modulators, broadband electromagnetic field sensors, and silicon-based photonic true time delay system.

Ching-Wen Chang received the B.S. degree in physics from National Sun Yat-sen University, Kaohsiung, Taiwan, in 2010, where she is currently working toward the Ph.D. degree with the Department of Physics. Her current research interests include the characterization of III–nitride semiconductor devices and molecular beam epitaxy technique.

Hai Yan received the B.S. degree in optical information science and technology from the Huazhong University of Science and Technology, Wuhan, China, in 2010, and the M.S. degree in electronic engineering from Tsinghua University, Beijing, China, in 2013. He is currently working toward the Ph.D. degree with the University of Texas at Austin, Austin, TX, USA. His research interests include silicon photonics, nonlinear optics, integrated photonic biosensors, and silicon-organic hybrid nanophotonic devices.

Ray T. Chen (M'91–SM'98–F'04) received the B.S. degree in physics from National Tsing Hua University, Hsinchu City, Taiwan, in 1980, the M.S. degree in physics, and the Ph.D. degree in electrical engineering, from the University of California, Oakland, CA, USA, in 1983 and 1988, respectively. He holds the Keys and Joan Curry/Cullen Trust Endowed Chair at The University of Texas (UT) at Austin, Austin, TX, USA. He is the Director of the Nanophotonics and Optical Interconnects Research Lab, the Microelectronics Research Center, The UT at Austin. He is also the Director of the newly formed AFOSR MURI-Center for Silicon Nanomembrane involving faculty from Stanford, UIUC, Rutgers, and UT Austin. He joined UT Austin in 1992 to start the optical interconnect research program. From 1988 to 1992, he was a Research Scientist, Manager, and the Director of the Department of Electro-Optic Engineering, Physical Optics Corporation in Torrance, CA, USA. He was the Chief Technical Officer (CTO), Founder, and Chairman of the Board of Radiant Research, Inc. from 2000 to 2001, where he raised 18 million dollars A-Round funding to commercialize polymer-based photonic devices involving more than 20 patents, which were acquired by Finisar in 2002, a publicly traded company in the Silicon Valley (NASDAQ: FNSR). He also was the Founder and Chairman of the Board of Omega Optics Inc. since its initiation in 2001. Omega Optics has received more than five million dollars in research funding. His research work has been awarded more than 120 research grants and contracts from such sponsors as Army, Navy, Air Force, DARPA, MDA, NSA, NSF, DOE, EPA, NIH, NASA, the State of Texas, and private industry. During his undergraduate years at the National Tsing Hua University, he led the 1979 university debate team to the Championship of the Taiwan College-Cup Debate Contest. He has supervised and graduated 50 Ph.D. students from his research group at UT Austin. The research topics are focused on three main subjects: first, Nanophotonic passive and active devices for sensing and interconnect applications, second, thin film guided-wave optical interconnection and packaging for 2-D and 3-D laser beam routing and steering, and third, true time delay wideband phased array antenna (PAA). Experiences garnered through these programs in polymeric and semiconducting material processing and device integration are pivotal elements for his research work. His group at UT Austin has reported its research findings in more than 780 published papers, including more than 85 invited papers. He holds 75 issued patents. He has chaired or been a program-committee member for more than 110 domestic and international conferences organized by IEEE, The International Society of Optical Engineering, OSA, and PSC. He has served as an Editor, Co-Editor, or coauthor for more than 20 books. He has also served as a Consultant for various federal agencies and private companies and delivered numerous invited talks to professional societies. He received the 1987 UC Regent's Dissertation Fellowship and the 1999 UT Engineering Foundation Faculty Award, for his contributions in research, teaching and services. He also received the honorary citizen award from Austin city council in 2003 for his community service contribution to black community, the 2008 IEEE Teaching Award, and the 2010 IEEE HKN Loudest Professor Award, 2013 NASA Certified Technical Achievement Award for contribution on moon surveillance conformable PAA. He is a Fellow of the OSA and SPIE.